$L(p)$ = differential operator as defined in Equation (1)
l_k = constants in system describing equation
M, $M(s)$ = Laplace transform of $m(t)$
$m(t)$ = manipulated, or control variable
M_j, $M_j(s)$ = Laplace transform of $m_j(t)$
$m_j(t)$ = signal obtained from $m(t)$
$\overline{m_j^2(t)}$ = mean square value of $m_j(t)$
N_d = NMP factors in G_d as defined in Equation (17)
N_p = NMP factors in G_p as defined in Equation (17)
P_{pd} = right-half plane poles of G_p not present as poles in G_d
p = poles
$Pr(\ )$ = probability of ( )
q = number of constraints
Q = portion of overall transfer function as defined in Equation (11)
$\hat{Q}$ = optimum Q
R, $R(s)$ = Laplace transform of set point
T = portion of overall transfer function as defined in Equation (49)
$\hat{T}$ = optimum T
t = time
$U(p)$ = differential operator as defined in Equation (1)
u_k = constants in Equation (1)
$\{V\}^+$ = portion of V having poles and zeros in the LHP
$\{V\}^-$ = portion of V having poles and zeros in the RHP
W_j^2 = mean-square constraint values of $m_j(t)$
z = zeros
Z_d = RHP zeros of G_d, $\prod_r (s + z_r)$, $z_r < 0$
Z_p = RHP zeros of G_p, $\prod_k (s + z_k)$, $z_k < 0$
$[\ ]_+$ = operation defined in Equation (33)
$[\ ]_-$ = operation defined in Equation (33)
$(\ )^*$ = complex conjugate

Greek Letters

ϵ = real and small constant
λ_j = Lagrangian multipliers
σ^2_{mj} = variance of $m_j(t)$
τ_d = dead time associated with G_d
τ_p = dead time associated with G_p
ϕ_{dd}, $\phi_{dd}(\tau)$ = autocorrelation function of $d(t)$
ϕ_{ee}, $\phi_{ee}(\tau)$ = autocorrelation function of $e(t)$
ϕ_{mm}, $\phi_{mm}(\tau)$ = autocorrelation function of $m(t)$
ϕ_{mjmj}, $\phi_{mjmj}(\tau)$ = autocorrelation function of $m_j(t)$
Φ_{dd}, $\Phi_{dd}(s)$ = spectral density of $d(t)$
Φ_{ee}, $\Phi_{ee}(s)$ = spectral density of $e(t)$
Φ_{mm}, $\Phi_{mm}(s)$ = spectral density of $m(t)$
Φ_{mjmj}, $\Phi_{mjmj}(s)$ = spectral density of $m_j(t)$
$\{\Phi_{dd}\}^-$ = portion of Φ_{dd} having poles and zeros in the RHP
$\{\Phi_{dd}\}^+$ = portion of Φ_d having poles and zeros in the LHP
ω = frequency

LITERATURE CITED

1. Newton, G. C., Jr., *J. Franklin Inst.*, **254**, 391 (1952).
2. Newton, G. C., Jr., L. A. Gould, and J. F. Kaiser, "Analytical Design of Linear Feedback Controls," pp. 34-38, 160-214, Wiley, New York (1957).
3. Chang, S. S. L., "Synthesis of Optimum Control Systems," pp. 63-99, McGraw-Hill, New York (1961).
4. Wiener, N., "Extrapolation, Interpolation and Smoothing of Stationary Time Series," pp. 84-86, Wiley, New York (1949).
5. Bendat, J. S., "Principles and Applications of Random Noise Theory," pp. 144-180, Wiley, New York (1958).
6. Horowitz, I. M., "Synthesis of Feedback Systems," pp. 495-524, Academic Press, New York (1963).
7. Lee, Y. W., "Statistical Theory of Communication," pp. 355-395, Wiley, New York (1960).
8. Seifert, W. W., and C. W. Steeg, "Control Systems Engineering," pp. 625-640, McGraw-Hill, New York (1960).
9. Merriam, C. W., III, "Optimization Theory and the Design of Feedback Control Systems," pp. 31-62, McGraw-Hill, New York (1964).
10. Luecke, R. H., and M. L. McGuire, *AIChE J.*, **14**, 173 (1968).
11. Hildebrand, F. H., "Methods of Applied Mathematics," pp. 121-168, Prentice-Hall, Englewood Cliffs, N. J. (1952).
12. Papoulis, A., "The Fourier Integral and its Applications," pp. 240-264, McGraw-Hill, New York (1962).
13. Brunk, H. C., "An Introduction to Mathematical Statistics," pp. 122-125, Ginn and Company, New York (1960).
14. Pugachev, V. S., "Proceedings Second IFAC Congress, Basle, Switzerland," Vol. 2, Pt. 2,1, Butterworths, England (1963).

Part II. Application to a Stirred Tank Reactor

The Wiener-Hopf procedure for synthesis of optimum constrained linear feedback regulators has been extended in part I to all linear time-invariant lumped parameter systems. The solution is here applied to the control of the output concentration of an exothermic, stirred tank reactor operating close to an unstable steady state, by constrained manipulation of a cooling water flow rate, in the presence of a randomly fluctuating inlet concentration.

When the spectral density of disturbance is given (for example, white noise through a first-order time delay, or a series of randomly alternating steps), the optimum controller has three modes: proportional, derivative, and integral with minor feedback. The responses of the nonlinear reactor and the linearized reactor control systems to a series of alternating deterministic step inputs and Gaussian distributed inputs are simulated, and a sensitivity study of the linearized system with respect to variations in process, controller, and disturbance parameters is made in order to demonstrate the feasibility of the method.

The identification of chemical systems from responses to random inputs has been examined by several authors (*1* to 5). More recently, the synthesis of optimum controllers by Wiener-Hopf methods for chemical systems subject to random disturbances has been treated (*6*, *7*).

In part I (*8*) of this two-part series, it was shown how to extend the Wiener-Hopf synthesis of optimum constrained linear feedback regulators to the general single-input, single-output linear, time-invariant system, with or without dead time. In this paper, the solution is applied to the control of the output concentration of an exothermic, stirred tank reactor in the presence of a randomly fluctuating inlet concentration. The reactor is to be operated close to its unstable steady state by manipulation of a constrained cooling water flow rate. Within a small operating region, the system dynamics may be represented by an unstable plant transfer function and an unstable, nonminimum phase disturbance transfer function. Therefore, the solution de-

veloped for case II in part I is directly applicable. Simulations of the original nonlinear reactor, as well as the linearized reactor with the optimum regulators, are presented. A sensitivity study of the linear system is also presented.

FORMULATION OF THE PROBLEM

Consider a stirred tank reactor (Figure 1) in which an exothermic reaction $A \rightarrow B$ is taking place with the rate $r_A = -k_0\, x \exp\,[-E_a/R_gT]x$, where x is the concentration of species A. This reactor is to be operated at its unstable steady state. It is desired to synthesize an optimum linear feedback regulator (Figure 2) to control the effluent concentration by manipulating the cooling water flow rate, within fixed limits, in the presence of a random inlet concentration disturbance.

The continuity and energy equations are

$$\frac{dx}{dt} = \frac{Q}{V_r}(x_i - x) - k_0 x \exp\,[-E_a/R_gT] \qquad (1)$$

$$\frac{dT}{dt} = \frac{Q}{V_r}(T_i - T) - \frac{k_0 x \exp\,[-E_a/R_gT]\Delta H}{\rho C_p} - \frac{UA(T - T_c)_m}{V_r \rho C_p} \qquad (2)$$

A steady state heat balance on the heat exchanger by assuming an arithmetic ΔT was used to eliminate $(T - T_c)_m$ in Equation (2), with the result

$$\frac{dT}{dt} = \frac{Q}{V_r}(T_i - T) - \frac{k_0 x \exp\,[-E_a/R_gT]\Delta H}{\rho C_p} - \frac{2\rho_c C_{pc} UA(T - T_{ci})Q_c}{V_r \rho C_p (2Q_c \rho_c C_{pc} + UA)} \qquad (3)$$

The usual linearization based on a Taylor series expansion of Equations (1) and (3) around its unstable steady state with appropriate numerical values given in Table 1 (9) yields

$$\frac{d\bar{x}}{dt} = 5.000 \times 10^{-3}\bar{x}_i - 1.316 \times 10^{-2}\,\bar{x} + 3.099 \times 10^{-3}\bar{Q} - 6.753 \times 10^{-5}\bar{T} \qquad (4)$$

and

$$\frac{d\bar{T}}{dt} = 5.000 \times 10^{-3}\bar{T}_i + 1.557 \times 10^{-2}\bar{T} - 2.69 \times 10^{-1}\bar{Q} + 1.940 \times 10^{-3}\bar{T}_{ci} - 1.029 \times 10^{-1}\bar{Q}_c + 2.719\bar{x} \qquad (5)$$

where the superbars are used to denote deviation variables from steady state. For the particular control scheme chosen, $\bar{Q}$, $\bar{T}_i$, and $\bar{T}_{ci}$ are zero. This reduces Equations (4) and (5) to

$$\frac{d\bar{x}}{dt} = 5.000 \times 10^{-3}\bar{x}_i - 1.316 \times 10^{-2}\bar{x} - 6.75 \times 10^{-5}\bar{T} \qquad (6)$$

and

$$\frac{d\bar{T}}{dt} = 1.557 \times 10^{-2}\bar{T} + 2.719\bar{x} - 1.029\bar{Q}_c \qquad (7)$$

Laplace transformation of Equations (6) and (7) and simultaneous solution of the resulting equations yields

$$\bar{x}(s) = \frac{6.954 \times 10^{-6}\bar{Q}_c(s)}{(s + 3.557 \times 10^{-3})(s - 5.969 \times 10^{-3})} + \frac{5.000 \times 10^{-3}(s - 1.557 \times 10^{-2})\,\bar{x}_i(s)}{(s + 3.557 \times 10^{-3})(s - 5.969 \times 10^{-3})} \qquad (8)$$

Equation (8) represents the dependence of the output concentration $x(t)$ in a small operating region of $Q_c(t)$ and $x_i(t)$. It is clear that this system is unstable, since it has a right-half plane (RHP) pole at $s = 5.969 \times 10^{-3}$, and the disturbance transfer function $\bar{x}(s)/\bar{x}_i(s)$ is nonminimum phase, since it has a RHP zero at $s = 1.557 \times 10^{-2}$. Physically, the latter implies that an increase in input concentration initially causes an increase in output concentration and temperature, but the corresponding increase in heat removal rate eventually drives both $x(t)$ and $T(t)$ below their initial values.

For convenience, we take the spectral density of the disturbance as

$$\Phi_{dd}(s) = \frac{4\mu^2}{(-s + 2\nu)(s + 2\nu)}; \quad s = i\omega \qquad (9)$$

which may represent a rectangular Poisson wave of constant or random magnitude, or Gaussian noise, obtained by passing white noise through a first-order delay element (transfer function). It may be noted that the spectral density is a rational function of s^2, which simplifies evaluation, and that any spectral density can be approximated by a sum of rational functions of s^2 (*10*).

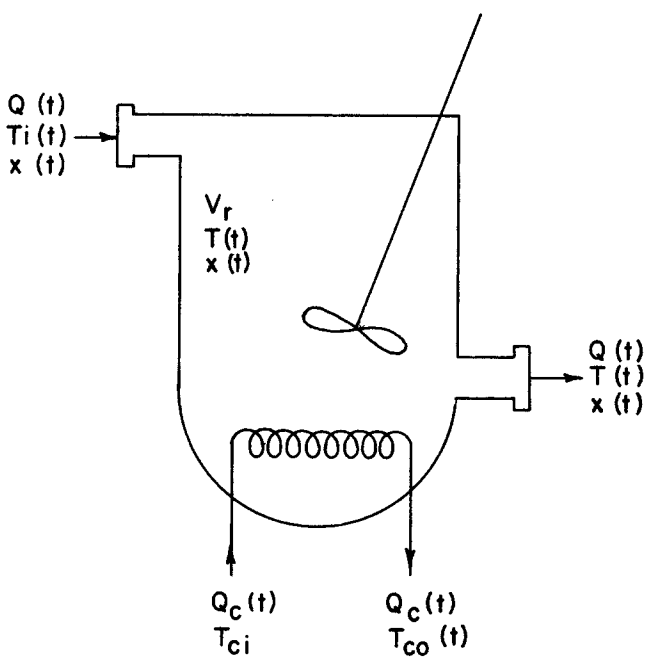

Fig. 1. Schematic diagram of stirred tank reactor.

OPTIMUM REGULATOR SYNTHESIS

From Equation (8), the system can be represented by the disturbance and plant transfer functions

$$G_d = \frac{a_1(s - a_2)}{(s - a_3)(s + a_4)}, \quad G_p = \frac{a_5}{(s - a_3)(s + a_4)}; \quad a_i > 0, \quad i = 1, 2, \ldots, 5 \qquad (10)$$

where G_d is unstable and nonminimum phase and G_p is unstable. In part I, the solutions for case II, which are preferred over those for case III for computational reasons, are given by Equations (39) and (40) for the optimum overall and controller transfer functions, respectively. For this system, we assume, without loss of generality, that

there is no dead time and that the measuring element is perfect; that is, $\tau_d = \tau_p = 0$ and $G_m = 1$. A statistical control effort constraint is given by

$$|m(t)| \leq a \tag{11}$$

which is to be satisfied over a specified fraction of time. Now the problem is to synthesize the optimum regulator shown in Figure 2 for the system of Equation (10), subject to a random disturbance, Equation (9), with a constraint given by Equation (11).

For this system

$$N_d = Z_d = (s - a_2);\ N_p = Z_p = 1;\ P_{pd} = 1;$$
$$G_m = 1;\ B_1 = 1;\ B_j = 0,\ j \neq 1$$

and

$$\{V\}^+ \{V\}^- = 1 + \left(\frac{\lambda}{a_5}\right)^2 (s - a_3)(s + a_4)(-s - a_3)(-s + a_4)$$
$$= \left(\frac{\lambda}{a_5}\right)^2 [(s + w_1)(s + w_2)(-s + w_1)(-s + w_2)] \tag{12}$$

where all constants are positive. Substitution of these terms into Equation (39), part I, yields the optimum transfer function

$$(\hat{C/D}) = N_d P_{pd} \hat{\bar{F}} = (s - a_2)\hat{\bar{F}}$$

$$= \frac{(s - a_2)\left[\lambda^2 \dfrac{2\mu\sqrt{\nu}}{s + 2\nu} \dfrac{a_1(s - a_2)}{(s - a_3)(s + a_4)} \cdot \dfrac{(s - a_3)(-s - a_3)(s + a_4)(-s + a_4)\left(\dfrac{a_5}{\lambda}\right)(-s - a_2)}{a_5 a_5 (s - a_2)(-s + w_1)(-s + w_2)}\right]}{\left(\dfrac{\lambda}{a_5}\right)(s + w_1)(s + w_2)(-s - a_2)\dfrac{2\mu\sqrt{\nu}}{s + 2\nu}}$$

$$= \frac{a_1(s - a_2)(s + 2\nu)}{(s + w_1)(s + w_2)(s + a_2)}\left[1 + \frac{f}{s + 2\nu} + \cdots\right]_+$$
$$= \frac{a_1(s - a_2)(s + g)}{(s + w_1)(s + w_2)(s + a_2)} \tag{13}$$

where

$$f = \frac{-(-2\nu + a_2)(-2\nu + a_3)(-2\nu + a_4)}{(2\nu + w_1)(2\nu + w_2)}$$

and

$$g = 2\nu + f \tag{14}$$

The optimum feedback regulator is given by

$$\hat{G}_c = \frac{G_d - (\hat{C/D})}{G_p(\hat{C/D})}$$
$$= \frac{(s + a_2)(s + w_1)(s + w_2) - (s + g)(s - a_3)(s + a_4)}{a_5(s + g)}$$
$$= K_p + K_d s + K_i/(s + K_f)$$
$$= K_c[1 + \tau_D s + K_I/(\tau_I s + 1)] \tag{15}$$

where

$$K_c = \frac{1}{a_5}[w_1 w_2 + a_2(w_1 + w_2) + a_3 a_4 + g(a_3 - a_4) - g(w_1 + w_2 + a_2 + a_3 - a_4 - g)]$$

$$\tau_D = \frac{1}{a_5}[w_1 + w_2 + a_2 + a_3 - a_4 - g)]/K_c$$

Table 1. Physical and Calculated Constants

a) Physical constants

$A = 500$ sq. ft.	$x_i = 0.5$ lb.-mole/cu. ft.
$k_0 = 3 \times 10^{11}$ sec.$^{-1}$	$Q_{css} = 0.6$ cu. ft./sec.
$C_p = C_{pc} = 1$ B.t.u./(lb.)(°R.)	$T_{iss} = 690$°R.
$V_r = 100$ cu. ft.	$T_{ci} = 520$°R.
$U = 100$ B.t.u./(hr.)(°R.)(sq. ft.)	$Q_{ss} = 0.5$ cu. ft./sec.
$\rho = \rho_c = 60$ lb./cu. ft.	$\Delta H = -2 \times 10^4$ B.t.u./lb.-mole
	$E_a = 4.45 \times 10^4$ B.t.u./lb.-mole

b) Calculated constants

Unsteady state conditions

Concentration, lb.-mole/cu. ft.	0.190
Temperature, °R.	716.9

$$\tau_I = 1/g$$

$$K_I = \left[\frac{1}{a_5}(a_2 w_1 w_2 + a_3 a_4 g) - K_c g\right] \Big/ K_c$$

$$K_p = K_c,\ K_d = K_c \tau_D,\ K_i = K_I K_c g,\ \text{and}\ K_f = \frac{1}{\tau_I} \tag{16}$$

It is interesting to note the form of the optimum regulator given by Equation (15), which is essentially a conventional PID controller. If g is very small, it reduces to an ideal PID controller. It can be anticipated that g will, in general, be small, corresponding to a small offset, according to the formula

$$\text{Offset} = \lim_{s \to 0} (\hat{C/D}) = \left(\frac{G_d}{1 + G_c G_p}\right)_{s=0}$$
$$= \frac{-a_1 a_2}{(-a_3 a_4 + a_5 k_c)d + a_5 k_c} = \frac{-a_1 g}{w_1 w_2} \tag{17}$$

This will be shown later to be, in fact, the case.

The solution is expressed in terms of w_1 and w_2, which are related to the system parameters and the Lagrangian multiplier λ by Equation (12). Since the unconstrained optimum in the configuration of Figure 2 calls for an infinite value of the manipulated variable, that is, $a = \infty$ in Equation (11), in practice the equality constraint equation

$$\frac{1}{2\pi i}\int_{-i\infty}^{+i\infty} \Phi_{mm}(s; w_1, w_2)\, ds$$
$$= \frac{1}{2\pi i}\int_{-i\infty}^{+i\infty} \left|\frac{(\hat{C/D}) - G_d}{G_p}\right|^2 \Phi_{dd}\, ds$$
$$= \frac{1}{2\pi i}\int_{-i\infty}^{+i\infty} \left|\left[\frac{a_1(s - a_2)(s + g)}{(s + w_1)(s + w_2)(s + a_2)}\right.\right.$$

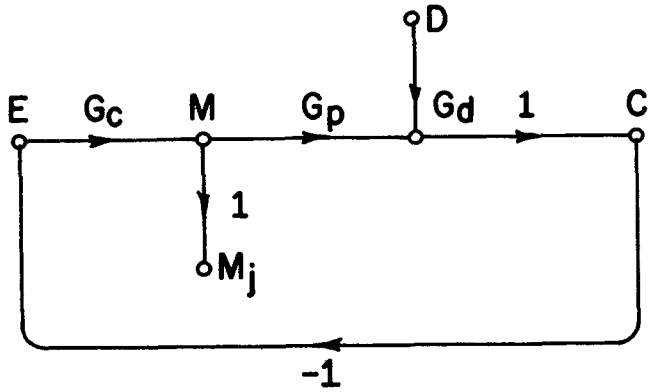

Fig. 2. Signal flow graph for regulation of stirred tank reactor.

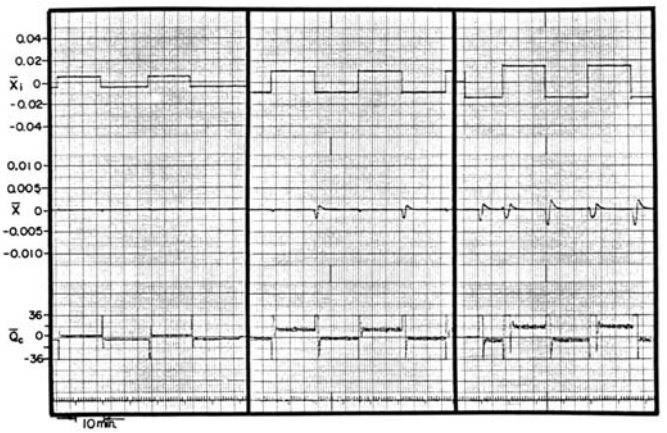

Fig. 3. Responses of nonlinear reactor control system to deterministic inputs.

$$\left. - \frac{a_1(s-a_2)}{(s-a_3)(s+a_4)} \right] \cdot \frac{(s-a_3)(s+a_4)}{a_5} \Bigg|^2 \frac{4\mu^2\nu}{-s^2+4\nu^2}\, ds$$

$$= I_4(w_1, w_2) = a/k \tag{18}$$

is imposed, where k is chosen in accordance with Table 1, part I. Two methods of solving Equation (18) can be used. One way is to assume a value for the Lagrangian multiplier λ in Equation (12) to obtain w_1 and w_2, since $w_1^2 + w_2^2 = a_3^2 + a_4^2$ and

$$(w_1 w_2)^2 = (a_3 a_4)^2 + (a_5/\lambda)^2 \tag{19}$$

where $\pm w_1$ and $\pm w_2$ are the roots of the polynomial equations

$$s^4 - (a_3^2 + a_4^2)\, s^2 + (a_3 a_4)^2 + (a_5/\lambda)^2 = 0 \tag{20}$$

These values of w_1 and w_2 are substituted into Equation (18). This process is repeated, presumably by a Fibonacci search (*11*), until Equation (18) is satisfied to within a specified error. Unfortunately, the expected range of values of λ is not usually known a priori. Alternatively, if w_1 and w_2 are complex, let

$$w_1 = re^{i\theta} \quad w_2 = re^{-i\theta} = w_1^* \tag{21a}$$

and for w_1 and w_2 real, let

$$w_1 = re^{\theta} \quad w_2 = re^{-\theta} \tag{21b}$$

In view of Equation (19) and (20), this is equivalent to defining θ by

$$\frac{p^2}{2q} = \begin{cases} \cos 2\theta & w_1, w_2 \text{ complex} \\ \cosh 2\theta & w_1, w_2 \text{ real} \end{cases} \tag{22}$$

where $p^2 = a_3^2 + a_4^2$; $q^2 = (a_3 a_4)^2 + (a_5/\lambda)^2$. Now, if the discriminant $(p^2/2)^2 - q^2 < 0$, corresponding to complex roots, then $0 \leq \cos 2\theta \leq 1$, so that $0 \leq \theta \leq \pi/4$. If $(p^2/2)^2 - q^2 > 0$, corresponding to real roots, then $0 \leq \theta \leq \frac{1}{2}\cosh^{-1}\left[\frac{a_3^2 + a_4^2}{2a_3a_4}\right]$, which is a consequence of taking the lower bound of q, corresponding to $\lambda = \infty$. These determine the range of θ to search in order to satisfy Equation (18). The solution can now be obtained by contour integration or by consulting tables (*12, 13*) or general expressions in a determinant form (*14, 15*). The integral in Equation (18) was evaluated from a table, along with the iteration method of Bolzano (*16*). By letting the equality constraint of Equation (18) be satisfied for $\theta = \theta_c$, it is readily seen that, for complex roots

$$r = \left(\frac{a_3^2 + a_4^2}{2\cos 2\theta_c}\right)^{1/2} \tag{23}$$

and

$$\lambda^2 = \frac{(2a_5 \cos 2\theta_c)^2}{(a_3^2 + a_4)^2 - (2a_3a_4 \cos 2\theta_c)^2} \tag{24}$$

while, for real roots

$$r = \left(\frac{a_3^2 + a_4^2}{2\cosh 2\theta_c}\right)^{1/2} \tag{25}$$

and

$$\lambda^2 = \frac{(2a_5 \cosh 2\theta_c)^2}{(a_3^2 + a_4^2)^2 - (2a_3a_4 \cosh 2\theta_c)^2} \tag{26}$$

NUMERICAL RESULTS

The following numerical results were obtained with the aid of the CDC-3400 digital computer and an EAI-680 analogue computer.

Optimum Controller and System Design

The optimum controller given by Equation (15) has three modes: proportional, derivative, and integral with a minor feedback (first order). Tables 2, 3, 4, and 5* show the effects on the optimum controller and system design of such factors as the mean frequency and mean disturbance amplitude, control variable amplitude constraint, and the probability of saturation. The numerical value of $K_f = 1/\tau_I$ is extremely small at low frequencies, and, therefore, in this low frequency range the optimum controller is essentially a PID controller. Equation (13) indicates that the optimum system has two zeros (one being an RHP zero) and three poles, of which two are a complex conjugate pair. Because of the RHP zero, the maximum phase lag is $-270°$. There are four parameters, of which two, the mean frequency and amplitude, ν and μ in Equation (9), are associated with the disturbance, while the remaining two, the constraint on $m(t)$ and the fraction of time the saturation is to be avoided, that is, a in Equation (11) and k in Equation (18), are at the disposal of the designer.

Table 2 shows that K_I is negative at frequencies higher than 0.01 crossings/sec. At these high frequencies, the

* Tables 3, 4, 5, 6, 7, and 8 have been deposited as document 00753 with the ASIS National Auxiliary Publications Service, c/o CCM Information Sciences, Inc., 22 W. 34th St., New York 10001 and may be obtained for $1.00 for microfiche or $3.00 for photocopies.

Table 2. Effect of the Mean Frequency of Disturbance on the Optimum Controller Design

$(\hat{C/D}) = a_1(s - a_2)(s + g)/[(s + w_1)(s + w_1^*)(s + a_2)]$, $\hat{G}_c = K_c\,[1 + \tau_D s + K_I/(\tau_I s + 1)]$

$\Phi_{dd} = 4\mu^2\nu/(\omega^2 + 4\nu^2)$, $\overline{Q_c^2(t)} = (a/3)^2$, $a = 0.6$, equivalent to 0.265% saturation probability based on a Gaussian distribution

μ = mean amplitude, lb.-mole/cu. ft.

$\lambda^2 \triangleq$ Lagrangian multiplier

ν = mean frequency, crossings/sec.

MSE $\triangleq$ mean-square error

μ	ν	$\lambda \times 10^3$	$Re(w_1) \times 10^2$	$Im(w_1) \times 10^2$	$K_c \times 10^{-2}$	τ_D	K_I	$\tau_I = \frac{1}{g}$	MSE $\times 10^6$	$I \times 10^6$
0.010										
	0.0010	0.566	177.0	7.83	20.7	12.0	5.700	505.00	0.0026	0.0154
	0.0050	14.0	7.26	1.53	0.903	63.3	0.216	97.10	1.63	9.47
	0.0075	17.1	6.03	1.38	0.626	74.1	0.140	66.20	3.16	14.8
	0.0100	16.6	6.21	1.41	0.581	71.3	−0.0952	52.90	3.72	14.7
	0.0500	5.90	17.1	2.40	1.72	15.2	−0.665	20.40	1.28	2.67
	0.1000	3.36	29.9	3.19	3.22	6.74	−0.775	14.80	0.551	1.00
	1.0000	0.524	185.0	7.99	20.7	0.541	−0.921	5.88	0.0248	0.0358
	5.0000	0.165	606.0	14.5	66.0	1.03	−0.954	3.30	0.0027	0.00379
0.015										
	0.0010					—*				
	0.0050					—				
	0.0075					—				
	0.0100	211.0	0.718	0.275	0.108	153.0	−0.259	56.2	205.00	1,985.0
	0.0500	16.0	6.590	1.45	0.959	14.2	−0.704	25.6	7.46	17.7
	0.1000	7.69	13.2	2.09	1.86	6.29	−0.776	18.9	2.51	4.87
	1.0000	1.03	97.4	5.80	11.9	0.534	−0.905	7.69	0.083	1.125
	5.0000	0.299	334.0	10.8	38.2	0.102	−0.939	4.33	0.0085	0.0121

* No feasible solution.

system phase lag is large, and an additional phase lag is introduced by the term $K_I/(\tau_I s + 1)$. This additional phase lag is not tolerable, and the amount is reduced by K_I taking on negative values. With an increase in the disturbance frequency, the mean-square error I, and λ at first increase and then decrease, exhibiting a maximum around 0.01 to 0.025 crossings/sec. This phenomenon may be explained from a Bode diagram of the optimum system, where the magnitude ratio is maximum at the resonance frequency. Hence, a disturbance whose frequency is close to the resonance frequency is difficult to handle, as indicated by the way the value of the Lagrangian multiplier changes with frequency. The numerical values of w_1 and w_1^*, the two closed-loop poles, show that at low and high frequencies the system stability is better than that at medium frequencies. Note that the optimum system tolerates an extremely small offset at all frequencies, due to the nonvanishing term of g. This is a characteristic of the spectral factorization technique. Physically, this implies that since the disturbance has a zero mean, the optimum system anticipates a change in sign and is hence willing to tolerate a small offset.

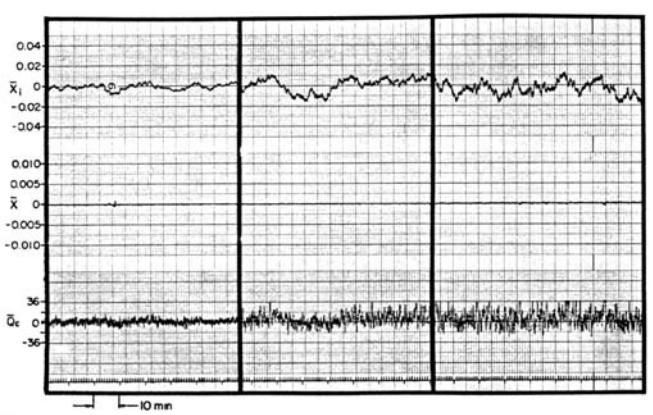

Fig. 4. Responses of nonlinear reactor control system to random inputs.

Table 3* shows that the MSE of the system increases, while the optimum controller gain K_c decreases with increasing amplitude. This is expected, since the larger the disturbance amplitude, the smaller will be the value of K_c in order to satisfy the constraint on the control variable. The Lagrangian multiplier increases with the mean amplitude, signifying an increase in the relative weighting assigned to the constraint.

In Tables 2 and 3,* some optimum controller parameters are omitted at some medium frequencies and at high mean amplitude. In these cases the synthesis resulted in extremely large K_c (such as 10^{21}) with resulting poor stability. Thus, these results indicate feasible design ranges for the given physical system and constraints.

Table 4* shows that better performance may be achieved by increasing the range within which the control variable is constrained, in the sense that the stability is improved and the MSE reduced. At high frequencies, these effects are much less apparent, since the power associated with the high frequency disturbance is small.

On the other hand, it is seen from Table 5* that the system can be designed to satisfy the magnitude constraint for a longer fraction of time at the expense of the MSE, although at some frequencies these seems to be an upper limit to this process. Note that the MSE given in the table is calculated on the basis of a linear system, with no saturation, and hence may not be a good approximation to the true MSE, which must be calculated from direct simulation. In order to maintain a high probability, the control effort is reduced, and consequently the MSE is in-

* See footnote on p. 243.

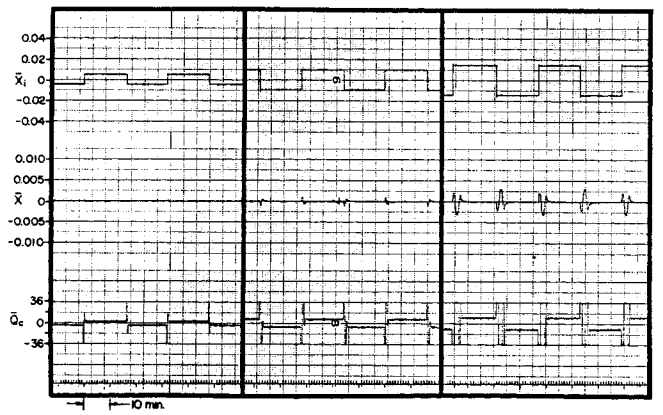

Fig. 5. Responses of linear optimum control system to deterministic inputs.

creased. The Lagrangian multiplier increases in value with a decrease in probability, giving more significance to the constraint at low probabilities of saturation.

Simulation of the Optimum Control System

The optimum controller design was based on a linearized model of the nonlinear reactor dynamic equations. To examine the errors thereby introduced, the linearized reactor model and the nonlinear model with the optimum linear feedback controller were simulated on an EAI-680 analogue computer. The disturbances in the feed concentration were series of alternating steps (deterministic) and a random input, with spectral density given by Equation (9), obtained by passing a white noise (Elgenco model 312A) with Gaussian distributed amplitude through a first-order delay element. The optimum controller with $K_c = 2{,}070$, $\tau_d = 12.0$, $K_I = 5.7$, and $\tau_I = 505$, corresponding to the case where $\mu = 0.01$ lb. mole/cu.ft., $\nu = 0.001$ crossings/sec., $a = 0.6$ cu.ft./sec., and $k = 3$ (0.265% saturation probability), was used.

The nonlinear reactor control system responses to alternating step and random changes in the feed concentration are given in Figures 3 and 4, respectively. In order to see how the system behaves when subjected to a range of disturbances, it was subjected to disturbances with mean amplitude equal to one-half, one, and two times the mean amplitude upon which the design was based. It is seen that the control is excellent, especially in view of a scale factor of 4 on the output over the input, so that on an equal scale basis the actual output is one-quarter of that shown. Note that the response of the system to a positive step change is much less than that to a negative step, an asymmetry typical of nonlinear systems. As expected, the

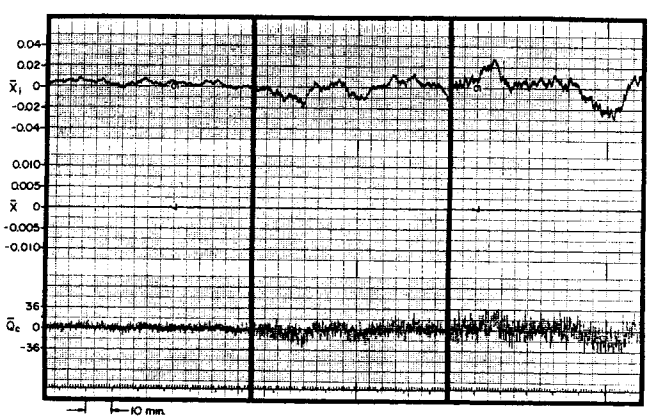

Fig. 6. Responses of linear optimum control system to random inputs.

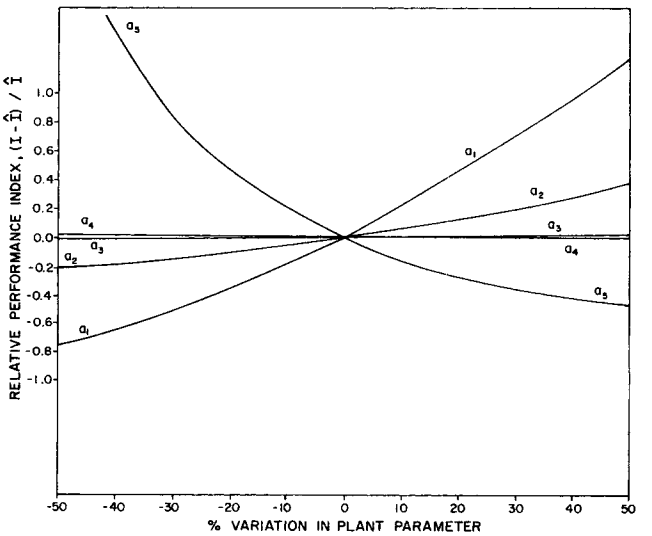

Fig. 7a. Sensitivity due to plant parameter variations. Effect on performance index.

control variable saturates when the disturbance is large. Also, the control variable is noisy, which is due to the presence of a derivative mode in the optimum linear regulator, Equation (15). This clearly demonstrates that the nonlinear reactor can be well regulated by the optimum linear regulator. Even though the system design is based on a random input, its response to a deterministic input is also excellent.

The responses of the linearized model reactor with the optimum regulator to random and alternating step changes in the inlet feed concentration are shown in Figures 5 and 6, respectively. Here again, disturbances with amplitudes one-half, one, and two times the nominal value were used. Since the overall system is essentially linear so long as the fraction of time saturation of control variable that takes place is negligible, the response amplitude is directly proportional to the disturbance amplitude. The quality of the control is again excellent.

Sensitivity Analysis

The performance of the actual control system will not be identical to that of the design, in view of the uncertainties and measurement errors in the system parameters. Sensitivity analysis can reveal how variations in the plant,

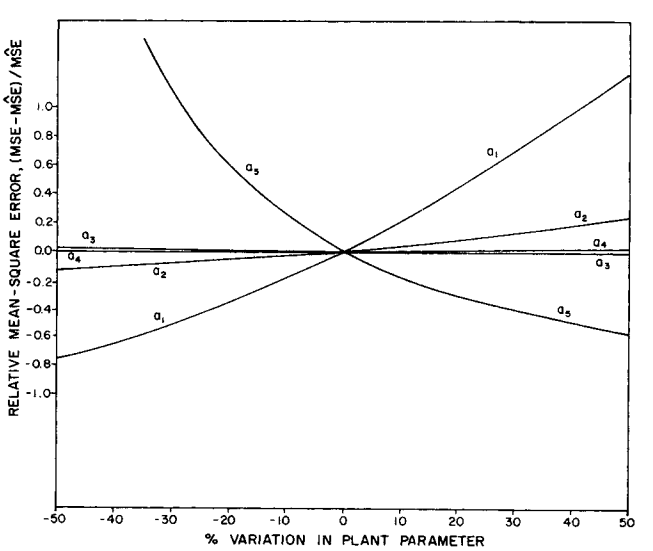

Fig. 7b. Sensitivity due to plant parameter variations. Effect on mean-square error.

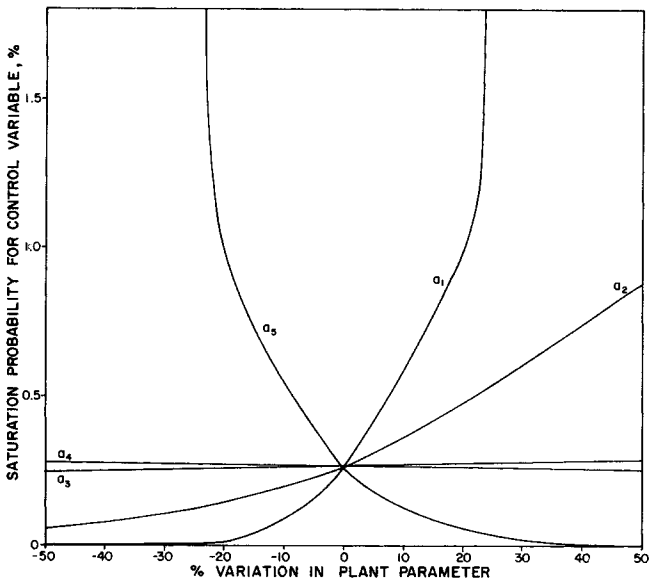

Fig. 7c. Sensitivity due to plant parameter variations. Effect on control variable saturation probability.

disturbance, and controller parameters change the control system characteristics, such as stability, performance index, MSE, and saturation probability.

A variational approach tends to be rather complicated, and a direct calculation of the desired system characteristics at various values of the plant, controller, and disturbance parameters was therefore performed. This study is based on the linear model.

Sensitivity due to Plant Parameter Variations. There are five parameters, a_i, $i = 1, 2, \ldots, 5$, which characterize G_d and G_p. By allowing variations only among these and by denoting the resulting new transfer functions by $\tilde{G}_d$ and $\tilde{G}_p$, the resulting overall system transfer function is

$$(\tilde{C}/D) = \tilde{G}_d/(1 + \hat{G}_c\, G_m\, \tilde{G}_p) \qquad (27)$$

whose characteristic equation determines the location of new closed-loop poles. Accordingly, the performance index is

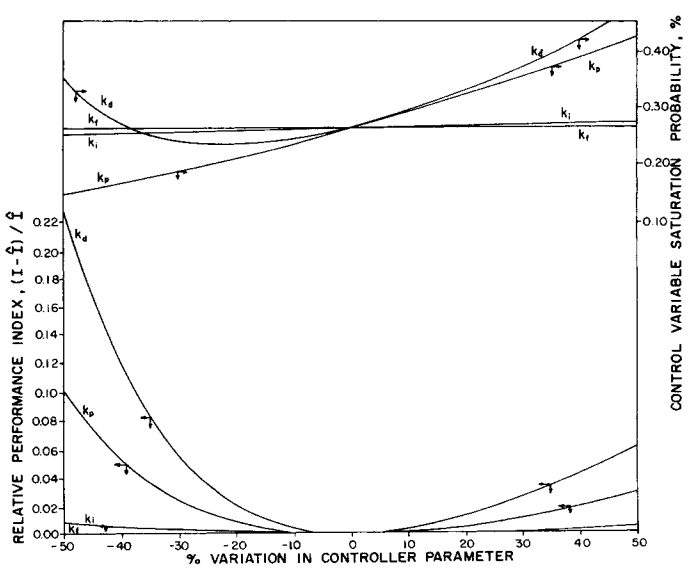

Fig. 8a. Sensitivity due to controller parameter variations. Effect on performance index and control variable saturation probability.

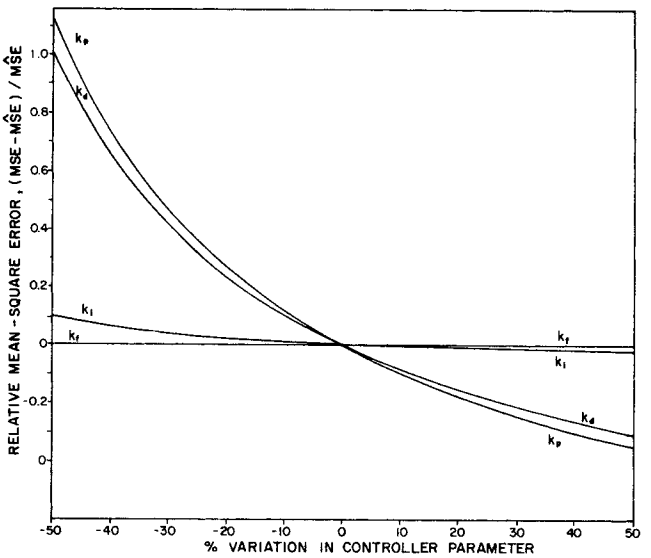

Fig. 8b. Sensitivity due to controller parameter variations. Effect on mean-square error.

$$\tilde{I} = \tilde{\phi}_{ee}(0) + \lambda^2\, \tilde{\phi}_{mm}(0)$$
$$= \frac{1}{2\pi i} \int_{-i\infty}^{+i\infty} (1 + |\lambda\, G_m\, \hat{G}_c|^2)\, |\tilde{G}_d/(1 + \hat{G}_c\, G_m\, \tilde{G}_p)|^2\, \Phi_{dd}\, ds \qquad (28)$$

where the MSE is given by the first term of the equation. The probability of saturation is also altered. For instance, for Gaussian signals

$$Pr(|m(t)| \leq a) = \text{erf}\left[a \Big/ \left(\frac{1}{\pi i} \int_{-i\infty}^{+i\infty} |\tilde{G}_d\, G_m\, \hat{G}_c/(1 + \hat{G}_c\, G_m\, \tilde{G}_p)|^2\, \Phi_{dd}\, ds \right)^{1/2} \right] \qquad (29)$$

The numerical results are given in Figures 7*a*, *b*, and *c* and Table 6,* where the variations represent deviations from the nominal values upon which the optimal synthesis was based. The parameters which affect the system characteristics least are the location of the left-half plane (LHP) and the RHP poles, a_3 and a_4. The optimum system is almost unaffected by ±50% variations in a_3 and a_4. The most pronounced effects are observed with variations in the gain of G_p, a_5, and in the gain of G_d, a_1, followed by variations in the RHP zero of G_d, a_2. Since $(C/D) = G_d/(1 + G_c\, G_m\, G_p)$ and $M/D = -G_c\, G_d\, G_m/(1 + G_c\, G_m\, G_p)$, positive variations in a_5 should decrease, while positive variations in a_1 and a_2 should increase the performance index, MSE, and probability of saturation. Figures 7*a*, *b*, and *c* bear out these expectations. Note that when the saturation probability is high, as in the cases of large negative variations in a_5 and large positive variations in a_1 and a_2, linear analysis is inappropriate, so that the calculated MSE may deviate considerably from the true MSE, which should be obtained through simulation. Variations in a_1 and a_2 do not alter the location of the closed-loop poles, whereas the variations in a_5 do. Thus, while the system is stable to ± 50% variations in all five parameters, it is expected from Equation (10) that large negative variations in a_5 or positive variations in a_1 and a_2 will impair the system characteristics. It may, therefore, be desirable to use a slightly lower value of a_5 and higher values of a_1 and a_2 than in the optimum synthesis. Table 6* shows how some joint variations affect the optimum system. Within ± 10% in individual variations the worst joint

* See footnote on p. 243.

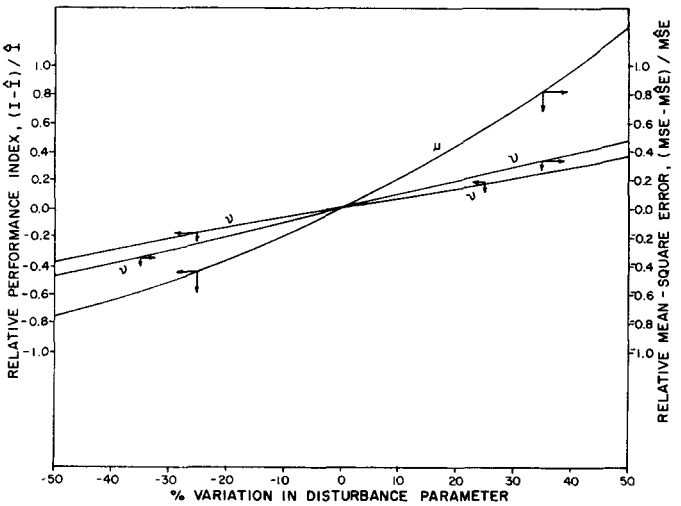

Fig. 9a. Sensitivity due to disturbance parameter variations. Effect on performance index and mean-square error.

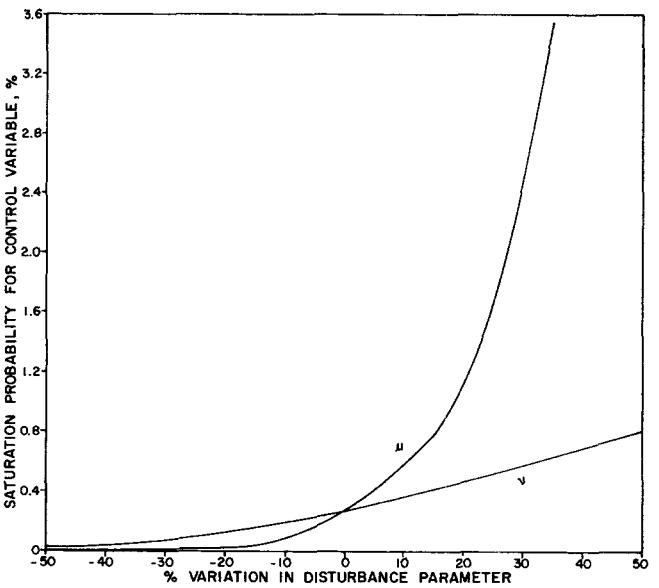

Fig. 9b. Sensitivity due to disturbance parameter variations. Effect on control variable saturation probability.

variation is a combination of -10% in the gain of G_p and $+10\%$ in the gain of G_d, which corresponds to overestimation of the control action and underestimation of the load effect.

It appears, therefore, that the resulting system is stable and that the performance characteristics are quite tolerant of deviations of the plant parameters.

Sensitivity due to Controller Parameter Deviations. We now vary the four parameters K_p, K_i, K_d, and K_f in the optimum controller given by Equation (15). Denoting by $\tilde{\hat{G}}_c$ the resulting nonoptimum controller, we see that the overall system transfer function is

$$(\tilde{C/D}) = G_d/(1 + \tilde{\hat{G}}_c\, G_m\, G_p) \tag{30}$$

whose characteristic equation determines the new location of the system poles. Accordingly, the performance index is also altered and is now given by

$$\tilde{I} = \tilde{\phi}_{ee}(0) + \lambda^2\, \tilde{\phi}_{mm}(0) = \frac{1}{2\pi i} \int_{-i\infty}^{+i\infty} (1 + |\lambda\, G_m\, \tilde{\hat{G}}_c|^2)|G_d/(1 + \tilde{\hat{G}}_c\, G_m\, G_p)|^2\, \Phi_{dd}\, ds \tag{31}$$

Note that the variations in the controller parameters represent deviations from the optimum settings and hence can only increase the performance index I of the resulting system. This fact can be used as means of checking the numerical result of the optimum synthesis. On the other hand, the MSE can either decrease or increase, depending upon whether the variations correspond to more or less control effort. This is also true for the probability of saturation, given by

$$\tilde{P}_r\,(|m(t)| \leq a) = \operatorname{erf}\left[a \Big/ \left(\frac{1}{\pi i} \int_{-i\infty}^{+i\infty} \left| \frac{G_d\, G_m\, \tilde{\hat{G}}_c}{1 + \tilde{\hat{G}}_c\, G_m\, G_p} \right|^2 \Phi_{dd}\, ds \right)^{1/2} \right] \tag{32}$$

As expected, the value of I is increased by all variations, as seen in Figure 8*a*. The probability of saturation increases, in general, with positive variations in K_p, K_i, and K_d. However, in general, the system characteristics are much less sensitive to controller parameter variations than to plant parameter variations. The increment in the performance index I is less than 2% for $\pm$ 20% variations in any of the controller parameters. The maximum deviation in the MSE is more substantial, 28%, but still much less than that due to plant parameter variations (Figure 8*b*). The variations in K_i and K_f, the two parameters associated with the integral mode $K_i/(s + K_f)$, have negligible effect on the system characteristics. Some joint effects are given in Table 7.* In general, positive variations reduce the MSE somewhat, at the expense of the probability of saturation. In summary, controller parameter variations only slightly affect the overall system characteristics.

Sensitivity to the Stochastic Disturbance Parameters. Consider now variations in the mean amplitude and frequency, u and ν, of the stochastic disturbance correlation function. It is clear that the overall system transfer function is not altered. The performance index is now given by

$$\tilde{I} = \tilde{\phi}_{ee}(0) + \lambda^2\, \tilde{\phi}_{mm}(0) = \frac{1}{2\pi i} \int_{-i\infty}^{+i\infty} [|\hat{C/D}|^2 + \lambda^2\, |(\hat{C/D})\, G_m\, \tilde{\hat{G}}_c|^2]\, \tilde{\Phi}_{dd}\, ds \tag{33}$$

and the saturation probability is given by

$$\tilde{P}\,(|m(t)| \leq a) = \operatorname{erf}\left[a \Big/ \left(\frac{1}{\pi i} \int_{-i\infty}^{+i\infty} (\hat{C/D})\, G_m\, \tilde{\hat{G}}_c|^2\, \tilde{\Phi}_{dd}\, ds \right)^{1/2} \right] \tag{34}$$

From Equations (9) and (33), positive variations in μ and ν increase the performance index I and the MSE $\tilde{\Phi}_{ee}(0)$, as indicated in Figure 9*a*. The probability of saturation follows the same pattern, as shown in Figure 9*b*. Some joint variations are shown in Table 8.* As expected, the more harmful variations of both u and ν are positive. For high saturation levels, the calculated MSE will be less than the actual. If a high level of saturation is undesirable, it may be necessary to overestimate u and ν, so that only negative variations will be anticipated.

* See footnote on p. 243.

CONCLUSIONS

A general solution for optimum regulators developed in part I is here applied to the control of the output concentration of a stirred tank reactor operating close to an unstable steady state. The numerical results for the optimum controller and system show a feasible range of design parameters. A simulation of both the original nonlinear reactor control system and of the linearized system with the linear optimum controller showed excellent response to either deterministic step or random inputs. A sensitivity study with respect to variations in the plant, controller, and disturbance parameters showed that the system can tolerate substantial uncertainties and offers some guide towards minimizing their effects.

ACKNOWLEDGMENT

Financial support by the Walter P. Murphy Foundation, the Union Carbide Company, the National Science Foundation (NSF Grant GK-1126), and the Ford Foundation is greatly appreciated. Thanks are also due to the Northwestern University Computing Center for providing a grant of computer time. Richard E. Kloubec of Purdue University performed the analogue simulations.

NOTATION

a, a_i = constants
B_j = Laplace transform of linear operator
C = Laplace transform of output $c(t)$
C_p, C_{pc} = heat capacity of feed and coolant, respectively
$(\hat{C/D})$ = optimum overall transfer function
$(\tilde{C/D})$ = overall transfer function resulting from parameter variation
D = Laplace transform of disturbance, $d(t)$
E = Laplace transform of error, $e(t)$
E_a = activation energy
$e(t)$ = error
f = constant
$\hat{F}$ = a portion of optimum overall transfer function (C/D)
g = constant
$\hat{G}_c$ = optimum controller transfer function
G_d = disturbance transfer function
G_m = transfer function of measuring element
G_p = plant transfer function
H = overall transfer function, (C/D)
I = Lagrangian function
k = ratio of instantaneous to root-mean-square constraints
k_0 = preexponential rate constant factor
M = Laplace transform of manipulated variable $m(t)$
M_j = Laplace transform of $m_j(t)$, $= B_jM$
$\overline{m^2(t)}$ = mean-square value for $m(t)$
N_d = nonminimum phase factors in G_d
N_p = nonminimum phase factors in G_p
p = constant
P_{pd} = RHP poles of G_p not present as poles in G_d
$Pr(\ )$ = probability of $(\ )$
q = constant
Q = feed flow rate
Q_c = coolant flow rate
$\overline{Q}_c(s)$ = Laplace transform of deviation of the coolant flow rate from the steady state value
R = Laplace transform of set point input function
R_g = universal gas constant
T = reaction fluid temperature
T_{ci} = inlet coolant temperature
T_{co} = outlet coolant temperature
T_i = inlet feed temperature
U = overall heat transfer coefficient
V_r = reactor volume
$\{V\}^+$ = portion of V having poles and zeros in the RHP
$\{V\}^-$ = portion of V having poles and zeros in the LHP
w_1, w_2 = constants
$\overline{x}(s)$ = Laplace transform of $\overline{x}(t)$
$x(t)$ = concentration
$\overline{x_i}(s)$ = Laplace transform of $\overline{x_i}(t)$
x_i = feed concentration
$[\ ]_+$, $[\ ]_-$ = operations defined in Equation (33), part I

Greek Letters

α = constant
β = constant
ΔH = heat of reaction
θ, θ_c = angles defined by Equations (21) to (25)
λ = Lagrangian multiplier
μ = mean amplitude of disturbance
ν = mean frequency of disturbance
ρ = reactant density
ρ_c = coolant density
τ_d = dead time associated with G_d
τ_p = dead time associated with G_p
Φ_{dd} = spectral density of $d(t)$
ϕ_{ee}, Φ_{ee} = autocorrelation and spectral density, respectively, of $d(t)$
ϕ_{mm}, Φ_{mm} = autocorrelation and spectral density, respectively, of $m(t)$
ω = frequency

Superscripts

* = complex conjugate
$\overline{\ }$ = deviation of time function from the steady state value
$\overline{\overline{\ }}$ = mean-square value
$\hat{\ }$ = optimum value
$\tilde{\ }$ = nonoptimum value resulting from parameter variations

LITERATURE CITED

1. Aris, Rutherford, and N. R. Amundson, *Chem. Eng. Sci.*, **9**, 250 (1957).
2. Homan, C. J., and J. W. Tierney, *ibid.*, **12**, 153 (1960).
3. Angus, R. M., and Leon Lapidus, *AIChE J.*, **9**, 810 (1962).
4. McCune, L. C., M. S. thesis, Northwestern Univ., Evanston, Ill. (1964).
5. Acrivos, Andreas, *Chem. Eng. Sci.*, **12**, 426 (1960).
6. Luecke, R. H., and M. L. McGuire, *AIChE J.*, **14**, 173 (1968).
7. *Ibid.*, 181.
8. Lim, H. C., and S. G. Bankoff, *AIChE J.*, **16**, 233 (1970).
9. Lim, H. C., Ph.D. thesis, Northwestern Univ., Evanston, Ill. (1967).
10. Lanning, J. H., Jr., and R. H. Battin, "Random Processes in Automatic Control," pp. 381-385, McGraw-Hill, New York (1956).
11. Johnson, S. M., *Rand Corp. Rept. P-856* (1956).
12. Chang, S. S. L., "Synthesis of Optimum Control Systems," pp. 345-346, McGraw-Hill, New York (1961).
13. Newton, G. C., Jr., L. A. Gould, and J. R. Kaiser, "Analytical Design of Linear Feedback Controls," pp. 372-381, Wiley, New York (1957).
14. Jury, E. I., and A. G. Dewey, *IEEE Trans. Auto. Control*, **AC-10**, 110 (1965).
15. *Ibid.*, 500.
16. Wilde, D. J., "Optimum Seeking Methods," p. 163, Prentice-Hall, Englewood Cliffs, N. J. (1964).

Manuscript received November 29, 1967; revision received August 23, 1968; paper accepted August 26, 1968. Paper presented at AIChE St. Louis meeting.